PERGAMON

International Journal of Multiphase Flow 26 (2000) 1905–1923

International Journal of Multiphase Flow

www.elsevier.com/locate/ijmulflow

On the interaction between two consecutive elongated bubbles in a vertical pipe

C. Aladjem Talvy, L. Shemer*, D. Barnea

Department of Fluid Mechanics and Heat Transfer, Faculty of Engineering, Tel-Aviv University, Tel-Aviv 69978, Israel

Received 3 August 1999; received in revised form 28 December 1999

Abstract

The motion of elongated air bubbles in a vertical pipe filled with water is studied quantitatively using video imaging of the flow and subsequent digital image processing of the recorded sequence of images. Experiments are carried out to determine the influence of the separation distance between two consecutive bubbles (liquid slug length) upon the behavior of the trailing bubble in vertical slug flow. The details of the trailing bubble acceleration and merging process are observed and the instantaneous parameters of the trailing bubble, such as its shape, velocity, acceleration, etc., are measured as a function of the separation distance. The leading bubble is found to be unaffected by the trailing elongated bubble.

Keywords: Two-phase slug flow; Image processing

1. Introduction

Slug flow is one of the basic gas–liquid flow patterns which takes place naturally inside pipes. It occurs over a wide range of flow parameters. The phenomenon of slug flow plays an important role in a variety of industrial applications.

Vertical slug flow is characterized by quasi-periodic alteration of large axisymmetric bullet-shaped (Taylor) bubbles and regions of continuous liquid phase, denominated liquid slugs, which may contain small bubbles. In developed slug flow, the Taylor bubbles occupy most of

* Corresponding author. Tel.: +972-3-640-8128; fax: +972-3-740-7334.
E-mail address: shemer@eng.tau.ac.il (L. Shemer).

0301-9322/00/$ - see front matter
PII: S0301-9322(00)00004-5

the pipe cross-section and move upward with a constant velocity. The liquid around the elongated bubbles moves downward as a thin falling film. The liquid velocity in the film is usually several times larger than the mean velocity of the liquid in the slug. Each slug sheds liquid in its back to the subsequent film, which accelerates as it moves downward. Then it is injected into the next liquid slug as a circular wall jet, producing a mixing zone in the bubble wake. The mixing zone is generally believed to have a shape of a toroidal vortex. The flow gradually reestablishes in the body of the liquid slug behind the mixing zone.

The translational velocity of a Taylor bubble, U_t, can be regarded as a superposition of its rise velocity in stagnant liquid U_0 and the contribution due to the mean liquid slug velocity U_M:

$$U_t = CU_M + U_0. \tag{1}$$

The drift velocity U_0 is determined by the three-dimensional flow at the front of the bubble. For the case of inertial flow (where both interfacial and viscous effects are negligible), Dumitrescu (1943) and Davies and Taylor (1949) showed that the drift velocity of an elongated bubble rising in a vertical pipe is

$$U_0 = k\sqrt{gD} \tag{2}$$

where the value of the coefficient k in Eq. (2) is about 0.35.

The value of the factor C in Eq. (1) is generally assumed to depend on the velocity profile in the liquid ahead of the bubble, and can be seen as the ratio of the maximum to the mean velocity in the profile. Hence, for turbulent flows, $C \cong 1.2$, while for laminar flow, $C \cong 2$ (Nicklin et al., 1962; Collins et al., 1978; Grace and Clift, 1979; Bendiksen, 1985).

Recently, Polonsky et al. (1999b) confirmed this assumption by performing direct PIV measurements of the velocity profiles ahead of the Taylor bubble, together with independent measurements of the bubble propagation velocity, in the entrance region of the pipe. The values of the coefficient C varies from 1.1 to 2.0. These values are in a good agreement with the measured ratio of the maximum to the mean velocity in the profile ahead of the Taylor bubble. Shemer and Barnea (1987) performed a visualization of the velocity profiles behind elongated bubbles and found that the tip of the trailing bubble in the wake of the leading one follows the location of the maximum instantaneous velocity in the wake.

For fully developed slug flow, the distance between any two consecutive bubbles is supposed to be large enough, so that the trailing bubble is uninfluenced by the wake of the leading one. However, in the entrance region of the pipe, the distance between the bubbles is not sufficiently large. The bubbles here are influenced by the flow in the wake of their predecessors, resulting in merging of bubbles and variation of the flow structure along the pipe (Moissis and Griffith, 1962; Taitel and Barnea, 1990). Similar effects are observed in two-phase flows in pipes laid over a hilly terrain (Zheng et al., 1994). The shedding rate of the liquid in the rear of the liquid slug seems to be larger for shorter slugs. As a results, the elongated bubble behind a short slug moves faster and overtakes the bubble ahead of it (Moissis and Griffith, 1962). This process decreases the slug frequency. The merging process continues until the liquid slug is long enough, so that the velocity of the trailing Taylor bubble is unaffected by the wake of the leading one.

Moissis and Griffith (1962), Taitel et al. (1980) and Barnea and Brauner (1985) assumed that the minimum stable slug length corresponds to the distance at which the liquid film is absorbed by the slug. They viewed this process as a wall jet entering a large reservoir. This approach provides an estimation of the average stable slug length, but tells nothing about the slug length distribution and the maximum possible slug length. As is well known, the slug lengths are widely dispersed around the average (Fabré and Liné, 1992; Van Hout et al., 1992). Barnea and Taitel (1993) presented a model that is capable of calculating the slug length distribution in a pipe. This model requires as input the dependence of the bubble translational velocity on the slug length ahead of it.

Hasanein et al. (1996) presented data on the rise velocity of the trailing Taylor bubble in air–kerosene slug flow as a function of the separation distance between the leading and the trailing bubbles. Pinto and Campos (1996) and Pinto et al. (1998) studied the coalescence of pairs of gas bubbles rising in vertical columns of liquids, covering a wide range of viscosities, by means of instantaneous pressure variation measurements at a number of locations along the pipe. Experimental results on the effect of the slug length on the velocity of the following bubble in a horizontal slug flow were reported by Netto et al. (1998).

In the present study, controlled experiments on the interaction between two consecutive elongated bubbles moving in a pipe are performed. The measurements are based on digital image processing of a recorded sequence of video images of the flow field. The application of this technique makes it possible to follow the instantaneous motion and the shape variation of the trailing elongated bubble as a result of the velocity field induced by the moving leading bubble. These observations are performed for the whole range of liquid slug lengths, starting from bubbles at a large separation distance up to the bubbles coalescence.

2. Experimental facility and procedure

Experiments are performed in a 4 m long transparent Perspex pipe with an internal diameter of 2.5 cm, see Fig. 1. A desired sequence of bubbles of prescribed lengths and intervals can be injected into the pipe that is filled with tap water. The pipe is equipped with three 1 m long rectangular transparent boxes filled with water in order to reduce image distortion. The flow field is illuminated by a number of halogen lamps. A vertical shaft provides support for two black-and-white interlaced NTSC video cameras located about 1.5 m from the pipe. The field of view of each camera is about 300×225 mm^2. The two fields of view overlap slightly. In order to obtain a better spatial resolution in the vertical direction, the cameras are rotated by 90°, so that the bubbles in the images appear to move horizontally. The distance over which the bubbles are followed by the two cameras consecutively is thus relatively long (~600 mm). On both sides of the test section, 500 W halogen lamps are mounted on folding support frames at the opposite sides of the test section. Tap water runs through the transparent boxes, so that the boxes are also used to cool the test section against the heat generated by the lamps. Constant temperature is therefore maintained during the experiment. The air supply system consists of an inlet air chamber and electrically activated valves. Air is supplied from a central compressed air line, at a nominal pressure of 0.6 MPa. The air inlet chamber is attached to the lower part of the test pipe at an angle of 30°. Individual bubbles are injected into the test pipe

by means of a computer-controlled injection valve. The valve, the chamber and the test section have the same inner diameter, in order to provide smooth entrance of air bubbles. The pressure in the air chamber is accurately monitored. The lengths of the injected bubbles are determined by the duration of the valve opening, which is controlled by the computer, as well as by the air pressure in the chamber. Synchronization that is required between the bubble injection, cameras switching and recording process is achieved using the PC-generated signals.

In the present study, pairs of elongated bubbles with various lengths and initial spacing are injected into stagnant water. The process of propagation, approach and eventual coalescence of the two bubbles is recorded by the computer using an appropriate custom-written software. The images are digitized at the rate of 30 frames/s, stored directly in the RAM of a personal computer and then transferred to a hard disk for permanent storage. The images are recorded only during the passage of the bubbles through the field of view of each camera. The portion of the image that contains the pipe with the bubbles is recorded in sequences of 100–150 frames for each series. The interlaced video images are then split into odd and even fields. The spacing between the lines is filled using linear interpolation between the gray levels in two adjacent lines. Hence, the effective rate of data acquisition is 60 images/s. More details about the experimental procedure and the data processing are given in Polonsky (1998) and Polonsky et al. (1999a).

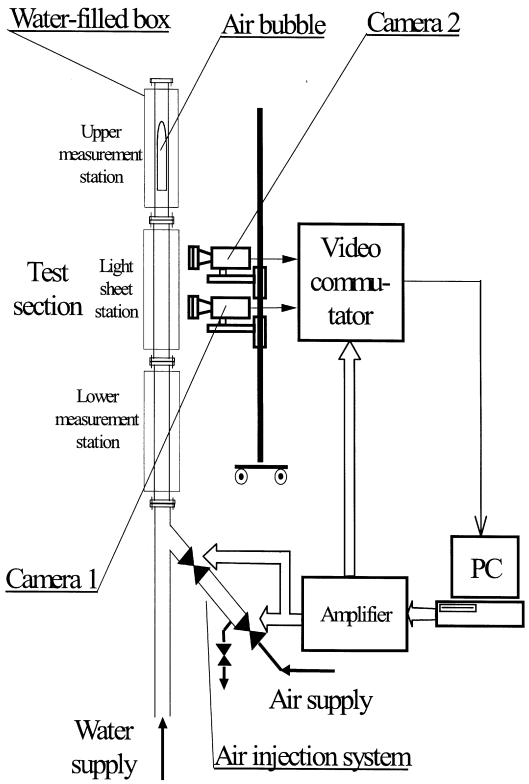

Fig. 1. Experimental facility.

An edge detection algorithm is then applied to detect the boundaries of the elongated bubbles present in each frame. An example of a resulting sequence of outlines of a bubble nose and bottom is presented in Fig. 2. The sequences of positions of the nose and the bottom outlines for a given bubble in the pth line of the qth image are saved separately in two arrays: $x_N(p, q)$ for the bubble's nose and $x_B(p, q)$ for the bubble bottom, see Fig. 3.

The local propagation velocity of the bubble interface (say, nose) at each radial location is calculated as the shift of the corresponding interface, divided by the time elapsed between the frames:

$$U_N^k(p, q) = \frac{x_N(p, q+k) - x_N(p, q)}{k\Delta t}. \tag{3}$$

In the above equation, the velocities are not necessarily calculated by comparison of consecutive profiles. Sometimes it is more convenient to consider the interface outlines for $k > 1$. This supplies a more robust averaged value of the interface velocity, especially when the shape of the outlines varies from frame to frame. The values obtained from Eq. (3) are first averaged over all radial positions (i.e. $1 < p < N_{rows}$) to obtain the instantaneous velocity averaged over the cross-section:

$$U_N = \frac{\sum_{p=1}^{N_{rows}} U_N^k(p, q)}{N_{rows}}. \tag{4}$$

The results are then averaged again for all the couples of images considered in the sequence of M outlines, in order to obtain the short-time averaged interfacial velocity.

For relatively large spacing between the two consecutive bubbles (exceeding about 5 pipe diameters), Eq. (4) is used to determine the instantaneous trailing bubble nose velocity. However, as shown in sequel, the nose of the trailing bubble may become very distorted in the near wake region of the leading bubble and does not retain a constant round and symmetric shape. The trailing bubble's tip may become sharp-pointed and ceases to be necessarily located at the pipe axis. Moreover, as a result of the distortion of the trailing bubble, its cross-sectional area may become strongly reduced. An alternative to (4) treatment should be thus applied to determine the instantaneous velocity of the trailing bubble nose. In the algorithm adopted here, the bubble tip coordinate $p_{tip}(q)$ is first determined for the qth nose outline. The bubble velocity at the instant t_q is defined by averaging the axial shifts of the nose outlines at n lines adjacent $p_{tip}(q)$ at both sides of the tip:

Fig. 2. Sequence of outlines: (a) bubble nose, (b) bubble bottom.

$$U_{\mathrm{N}}(q) = \frac{\sum_{j=-n}^{n} \left\{ x_{\mathrm{N}}\left[p_{\mathrm{tip}}(q+k)+j\right] - x_{\mathrm{N}}\left[p_{\mathrm{tip}}(q)+j\right] \right\}}{(2n+1)\cdot k \cdot \Delta t} \tag{5}$$

Averaging of Eq. (5) over a desired number of the nose outlines can then be performed. The separation distance between the two bubbles is calculated as the difference between the averaged instantaneous coordinate of the leading bubble bottom and the instantaneous trailing bubble tip location.

3. Results

In each experimental run, a couple of bubbles of a prescribed length and initial spacing between them is injected into the pipe. The experiments cover a wide range of distances between bubbles (from 60 pipe diameters, D, to coalescence). For the whole range of separation distances, Taylor bubbles of different lengths are tested: short (1–2D), medium (6–7D) or long (11–12D).

An example of a recorded series of two interacting bubbles, of about 6D long each, is given in Fig. 4. The sequence of frames is obtained after separating of the odd and the even fields in the interlaced image, thus corresponding to a time interval of 1/60 s between the images. The motion and the shape of the trailing bubble are strongly affected by the wake of the leading one, eventually leading to the bubbles merging. The stage of full merging, where a single long bubble is eventually obtained, is not shown in Fig. 4. Yet, the rise velocity of the leading bubble bottom in Fig. 4 appears to be completely undisturbed by the approaching trailing bubble, even when the coalescence is imminent. Consecutive outlines of the leading Taylor bubble nose, as well as the trailing bubble nose, are presented in Fig. 5. This figure demonstrates that while the outlines of the leading rising Taylor bubble are equidistantly distributed and remain round shaped; the trailing bubble nose interfaces do not retain a constant shape due to the influence of a leading bubble wake.

3.1. Leading bubble motion

The instantaneous velocities of the leading Taylor bubble nose for separation distances

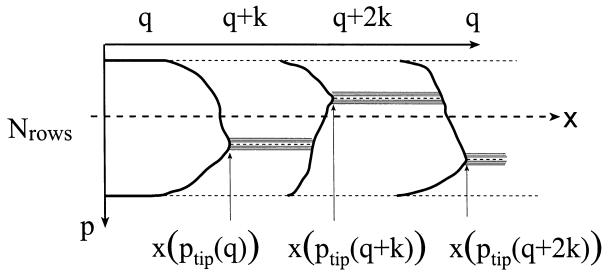

Fig. 3. Coordinate system for the determination of the instantaneous bubble outline.

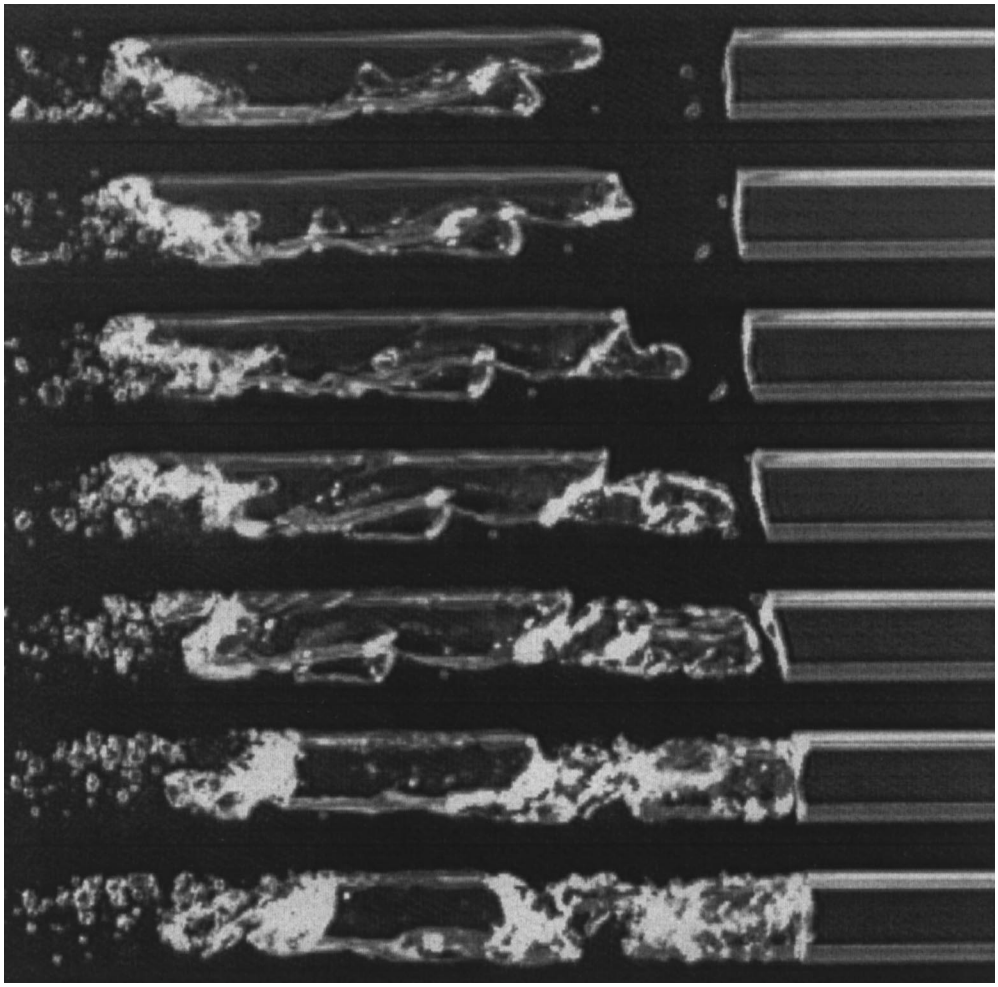

Fig. 4. Example of a recorded sequence of two consecutive bubbles.

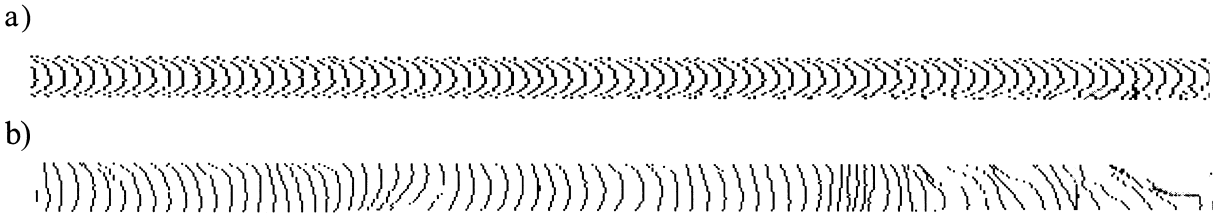

Fig. 5. A sequence of instantaneous nose outlines up to coalescence: (a) leading bubble, (b) trailing bubble.

ranging from more than 6*D* up to coalescence are plotted in Fig. 6. The rise velocity of the leading bubble in Fig. 6 apparently remains constant throughout the whole process of bubbles approach and coalescence.

A salient feature of a single Taylor bubble motion in a vertical pipe is the quasi-periodic oscillations of the bubble bottom. Polonsky et al. (1999a) reported that the frequency of the dominant mode of the interface oscillations obtained experimentally in the present facility is about 3–4 Hz. A simple theoretical model presented in their paper yields a similar value. The frequency of the dominant mode of the bottom oscillations of the leading bubble in the presence of the trailing one is examined here as well. The oscillations of the leading bubble bottom interface are analyzed in a sequence of frames where the trailing and the leading bubbles approach and eventually merge. A comparison of the spectrum of the leading bubble bottom oscillations with that of a single Taylor bubble is presented in Fig. 7. The spectrum in both cases has a well-pronounced resonant character, with close values of the dominant frequency.

It can thus be concluded that in the sequence of two interacting bubbles in stagnant water, the trailing Taylor bubble does not affect the motion of the leading Taylor bubble. A uniform rising velocity of the leading bubble is therefore assumed in the course of the data processing in the present study. Moreover, since the effect of bubble expansion is relatively weak (Polonsky et al., 1999a), it is assumed here that the nose and bottom of the leading bubble propagate with identical velocities.

3.2. Trailing bubble motion

The motion of the trailing bubble is strongly affected by the wake of the leading Taylor

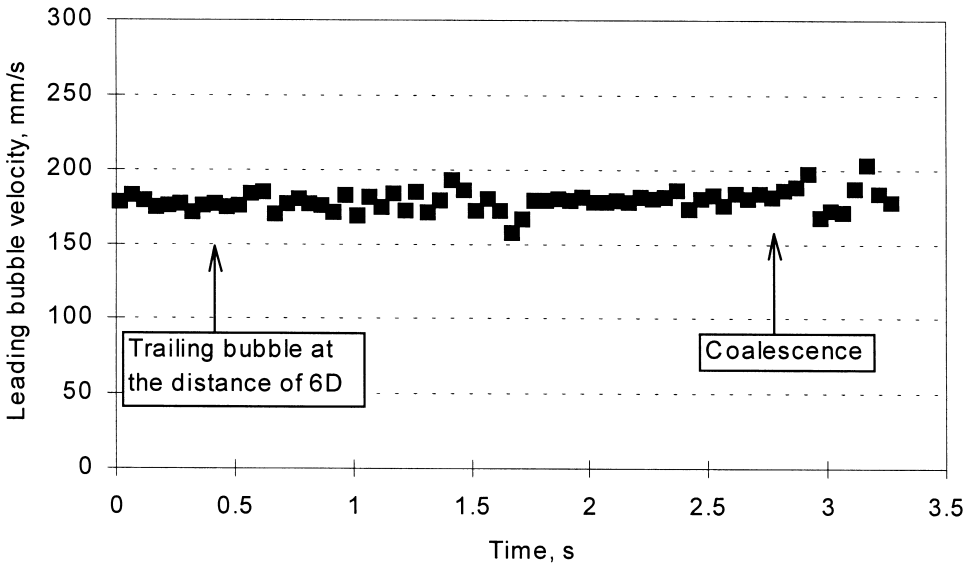

Fig. 6. The leading bubble rise velocity obtained at different stages of the two bubbles approach.

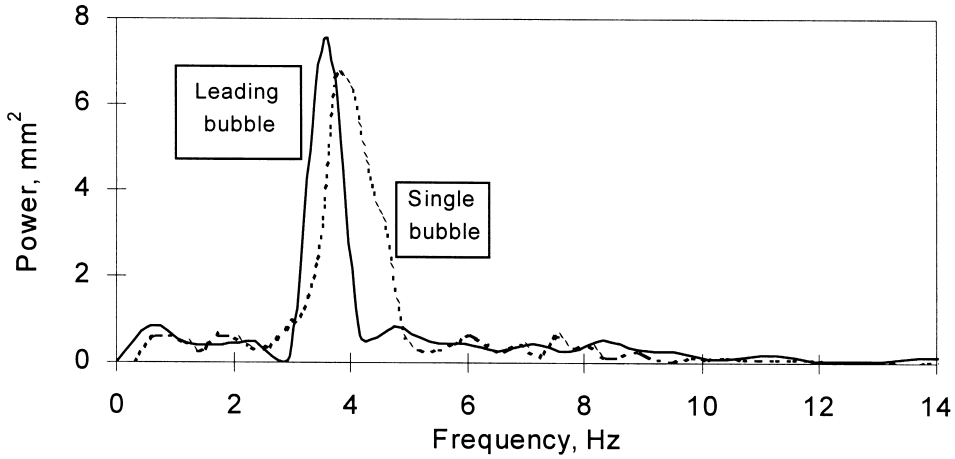

Fig. 7. Spectra of the bubble bottom oscillations for a single Taylor bubble and for the leading bubble just before coalescence.

bubble. Figs. 4 and 5 clearly demonstrate that the trailing bubble's nose is deformed and its shape changes rapidly in the course of the bubble approach. An additional sequence of recorded images in Fig. 8 presents a relatively short trailing bubble in a frame of references moving with a constant velocity of the leading bubble. In this case, the trailing bubble's nose is strongly accelerated, while its tail moves with a nearly constant velocity. The bubble becomes

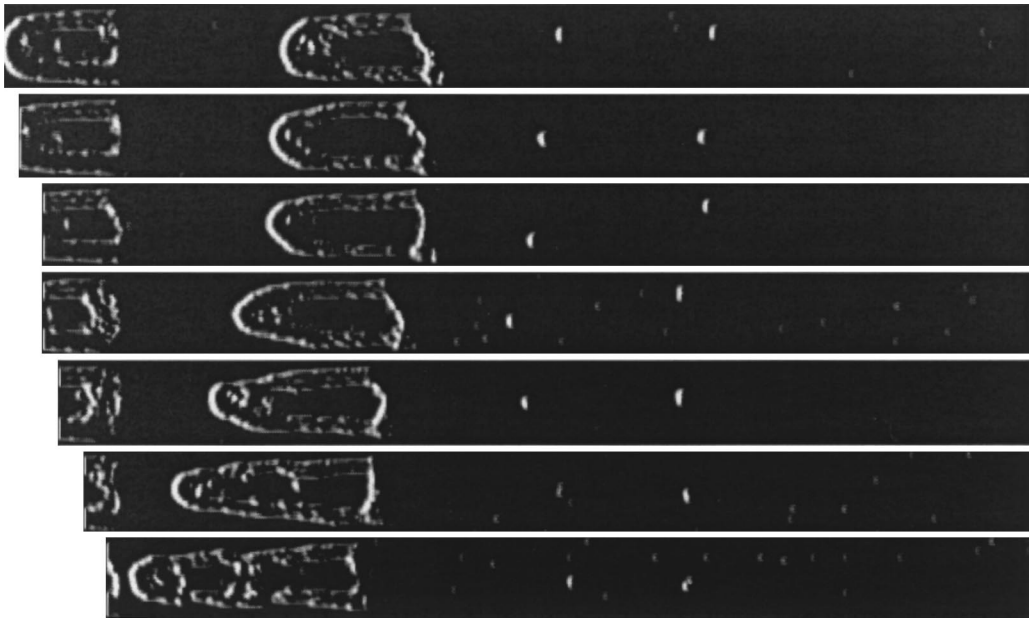

Fig. 8. Deformation of the trailing elongated bubble prior to coalescence with the leading one. Time separation between the images 1/30 s.

substantially longer as it approaches the leading bubble, and the liquid film around the bubble becomes quite thick. The radial location of the bubble tip varies notably from frame to frame. In the last frame of Fig. 8, splitting of the bubble into two separate bubbles is clearly seen. Disintegration of the trailing bubble is also observed in Fig. 4. Note that in Fig. 8 two small bubbles are seen in the wake of the trailing bubble. The distance between these two bubbles increases first and then decreases. The distances between each one of the small bubbles and the elongated one also vary in a complicated fashion, thus providing a clear demonstration of the complexity of the velocity field in the elongated bubble's wake. The complicated nature of the trailing bubble motion as recorded in Figs. 4 and 8 justifies the different definition of the trailing bubble velocity in the previous section.

Sequences of the trailing bubble's nose outlines are presented in Fig. 9 for various instantaneous separation distances between the bubbles. As long as the length of the liquid slug ahead of the trailing bubble is relatively large (about $7D$), the consecutive bubble's nose shapes remain nearly symmetric and equidistant. When the liquid slug separating the bubbles becomes shorter, the bubble nose becomes strongly distorted due to the effects of the vortical flow field in the leading bubble wake. The trailing bubble's tip starts "swinging" from one side of the pipe to the other, and the distance between consecutive nose outlines becomes strongly dependent on the radial location. Fig. 9 demonstrates that the oscillations of the nose become stronger as the liquid slug becomes shorter. A notable increase in the trailing bubble velocity as it approaches the leading bubble can be seen in Fig. 9c.

The Taylor bubble propagation velocity in the wake of the leading one is determined by the local instantaneous velocity at the bubble tip (Polonsky et al., 1999b). In an unsteady flow, the term CU_M in Eq. (1) can thus be replaced by the instantaneous liquid velocity at the bubble tip. Shemer and Barnea (1987) and Polonsky et al. (1999b) suggested that trailing bubble tip follows the location of the maximum liquid velocity in the profile ahead of the bubble.

The temporal variation of the instantaneous radial position of the tip of the trailing bubble nose is plotted in Fig. 10. The increase in the amplitude of the nose tip oscillations with

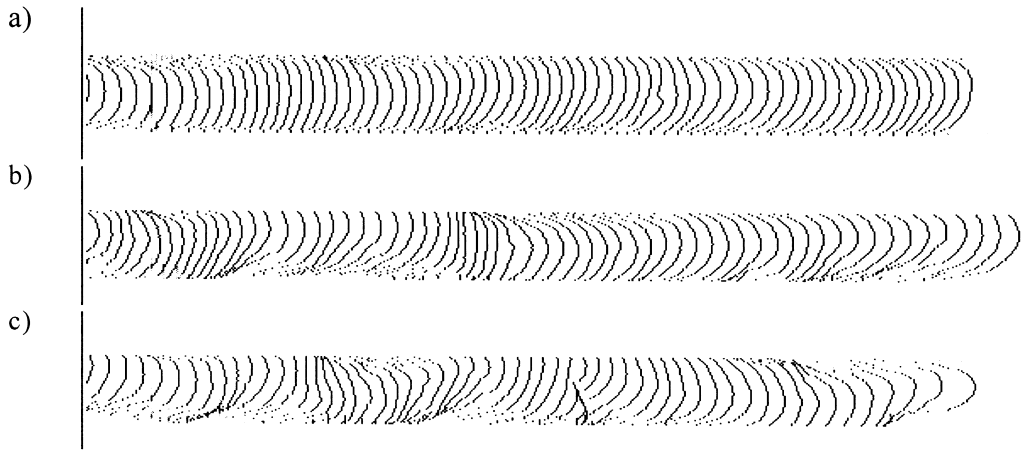

Fig. 9. Trailing bubble nose outlines: (a) 7 to $5.5D$ behind the leading bubble; (b) 6 to $4.5D$ behind the leading bubble; (c) 4 to $2D$ behind the leading bubble.

decreasing distance between the bubbles is clearly demonstrated in this figure. It should also be noted here that the characteristic frequency of the quasi-periodic nose tip oscillations is close to the peak frequency in the leading bubble bottom oscillations in Fig. 7. This suggests that the instantaneous rate of the trailing bubble propagation is controlled to a certain extent by the quasi-periodic oscillations of the bottom of the leading bubble and the velocity field induced in the leading bubble wake by those oscillations.

Based on the known location of the bubble tip, the instantaneous trailing bubble approach, or relative, velocity (i.e. the difference between the varying trailing bubble velocity and the constant leading bubble velocity) can be determined using Eq. (5) with $n = 5$ and $k = 1$. The fluctuations of the liquid velocity ahead of the trailing bubble can either accelerate the bubble propagation or slow it down, depending on the instantaneous location of the bubble tip and the sign of the fluctuation of the axial velocity. Since the intensity of these fluctuations varies significantly with the distance from the leading bubble bottom, the distance to the leading bubble apparently strongly affects the variations in the trailing bubble velocity. The oscillations of the trailing bubble velocity, therefore, become more violent as the trailing Taylor bubble approaches the leading one. Fig. 11 demonstrates the patterns of the relative velocity behavior as a function of the distance between the bubbles. Each frame in this figure represents a single realization. Even at a considerable separation distance (Fig. 11a), notable oscillations of the instantaneous velocity are seen. The mean value for this realization is clearly positive, about 10 mm/s. As the spacing becomes shorter (Fig. 11b), the velocity fluctuations increase significantly in amplitude. The mean velocity is clearly positive, but at some instants the approach velocity can become negative. This feature is even more pronounced in the near wake region (Fig. 11c and d).

The measured instantaneous approach velocity of the trailing bubble just prior to coalescence is presented in Fig. 12. Again, as in Fig. 11, the rate of approach may locally become negative, but on the average, the acceleration towards the leading bubble is extremely high: just before coalescence, the trailing bubble can attain velocities exceeding 1 m/s, more than seven times that of the leading bubble. Note that the images of Fig. 4 demonstrate that

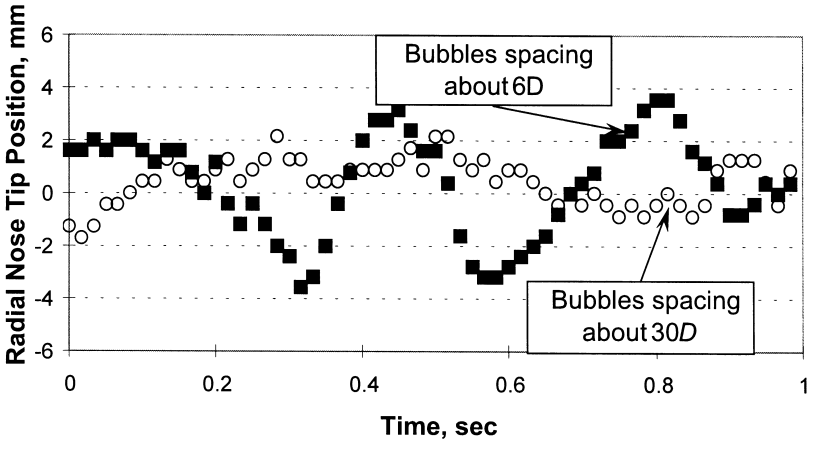

Fig. 10. Radial oscillations of the trailing bubble tip at two distances from the leading Taylor bubble.

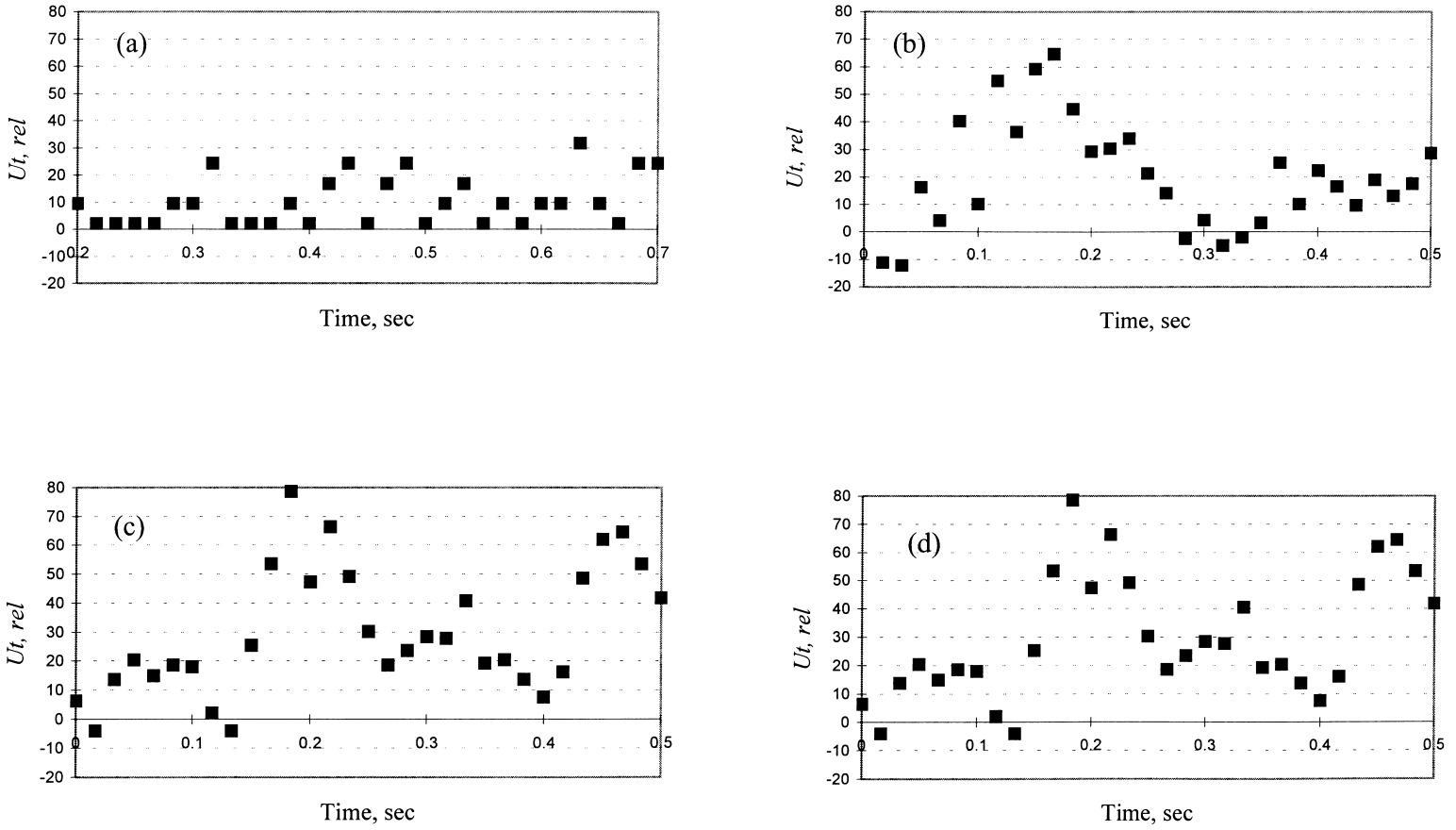

Fig. 11. Variation of the instantaneous trailing bubble velocity relative to the leading one. Separation distance between bubbles: (a) 36D, (b) 6D, (c) 4D, (d) 3.7D.

the interface between the elongated bubbles does not disappear immediately after the nose of the trailing bubble becomes attached to the bottom of the leading one, rather, a film separating the bubbles remains clearly visible for a number of frames. The two bubbles thus propagate for some time with the velocity of the leading bubble, before fully merging.

In Fig. 13, histograms representing the frequencies of appearance of the instantaneous approach velocities of bubbles of intermediate length (about $6D$) are given for three ranges of the bubble spacing. For each bubble spacing range, the ensemble size is about 1000. As the distance between the bubbles decreases, the distributions slide to the right, in the direction of higher trailing bubble propagating velocities, and the dispersion of the data becomes wider.

Fig. 13 further supports the observation (Fig. 11) that interaction between bubbles apparently exists at distances exceeding what was previously considered to be "a stable liquid slug length". In vertical slug flow, the stable liquid slug length is assumed to be around $16D$ (Moissis and Griffith, 1962), yet, the experimental results in Fig. 13 indicate an average positive rate of approach for much larger spacings between bubbles. In other words, two Taylor bubbles in stagnant water that are separated initially by a liquid slug of length of about $60D$, will end up colliding, provided the pipe is sufficiently long.

The effect of the bubble length on the interaction phenomenon is now studied. The results of Polonsky et al. (1999a) revealed an increase in the intensity of the bubble bottom oscillation with the increase in the bubble length. It is thus logical to assume that the intensity of the velocity fluctuations in the wake of a Taylor bubble is higher for longer bubbles, with a corresponding effect on the motion of the trailing bubble.

The following lengths were chosen for the study of the interaction between couples of Taylor bubbles: (i) short Taylor bubbles ($1–2D$), (ii) bubbles of an intermediate length, ($6–7D$) and (iii) long bubbles ($11–12D$). Above this length, the increase in the intensity of the bubble bottom oscillations is no longer significant (Polonsky et al., 1999a).

The histograms presented in Fig. 14 shows the frequency of appearance of different values of

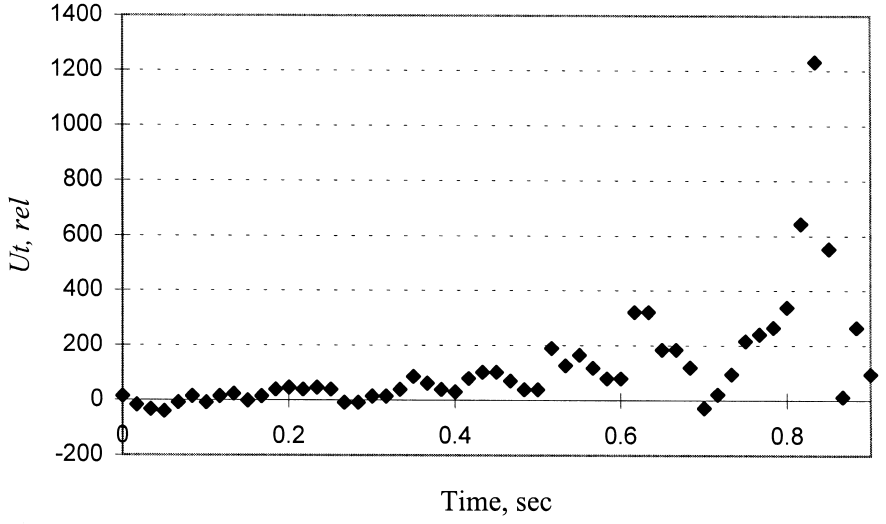

Fig. 12. Instantaneous relative velocity of the trailing bubble. Separation distance from $3D$ up to coalescence.

the relative velocity. The distributions are given for the three cases of bubble lengths (1*D*, 6*D* and 12*D*). For each range of bubble lengths, the total ensemble of experimental data accumulated varies from 1000 to 2000 values. The frequency of the different values of the relative velocity is normalized by the total size of the corresponding ensemble to enable comparison. Fig. 14 reveals that at different stages of the pursuit, the dispersion in the data of the bubbles relative velocity is higher for longer bubbles. The histograms also tend to slide to the right for longer bubbles. These results indicate that for a given spacing between the bubbles, the acceleration of the trailing bubble is somewhat higher for longer bubbles.

The considerable amount of data gathered in this study makes it possible to calculate the average trailing bubble propagation velocity for various bubble separations and various bubble lengths. Fig. 15 presents the variation of the averaged trailing bubble velocity with the separation distance for two different lengths of the bubbles in each couple. The trailing Taylor bubble velocity is normalized here by that of the leading one. Two different scales are applied for the larger and shorter separation distances. Notable acceleration of the trailing bubble is observed at distances shorter than about 3D (Fig. 15a). As could be expected, this acceleration

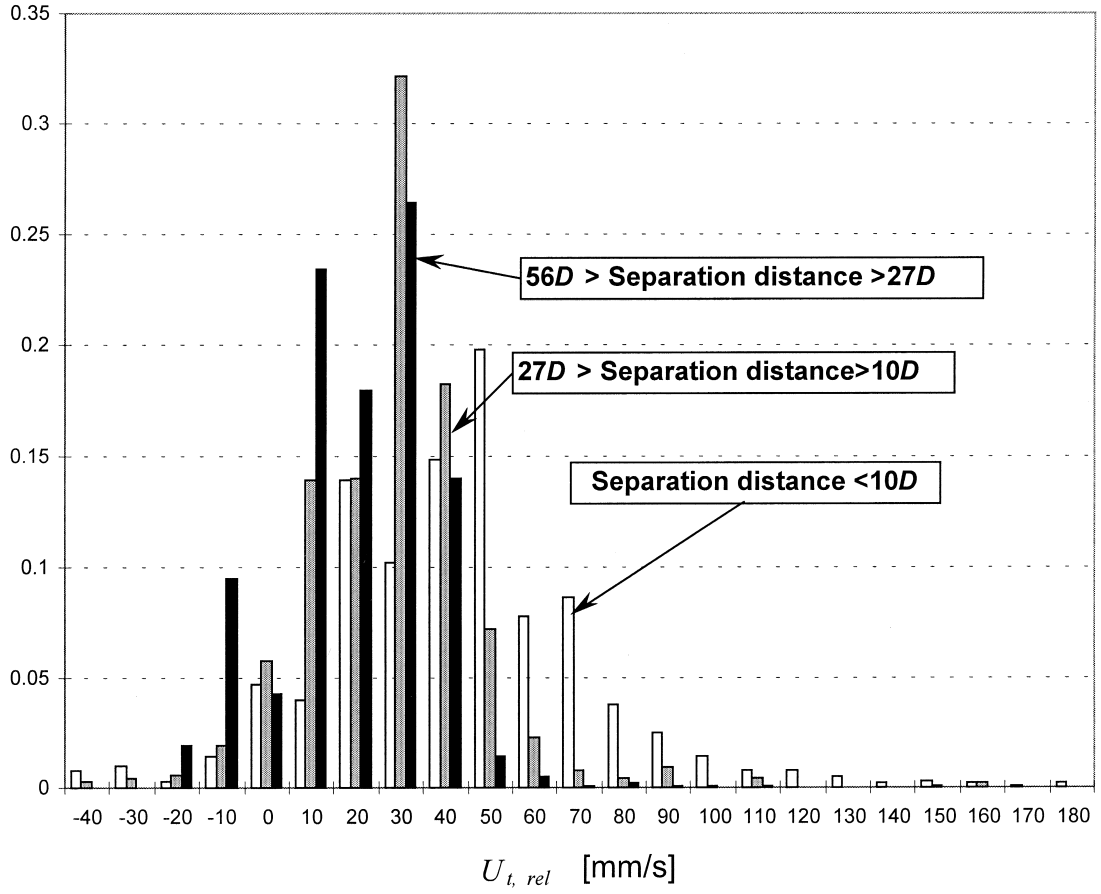

Fig. 13. Histograms of the instantaneous relative velocity of the trailing bubble at various separation distances.

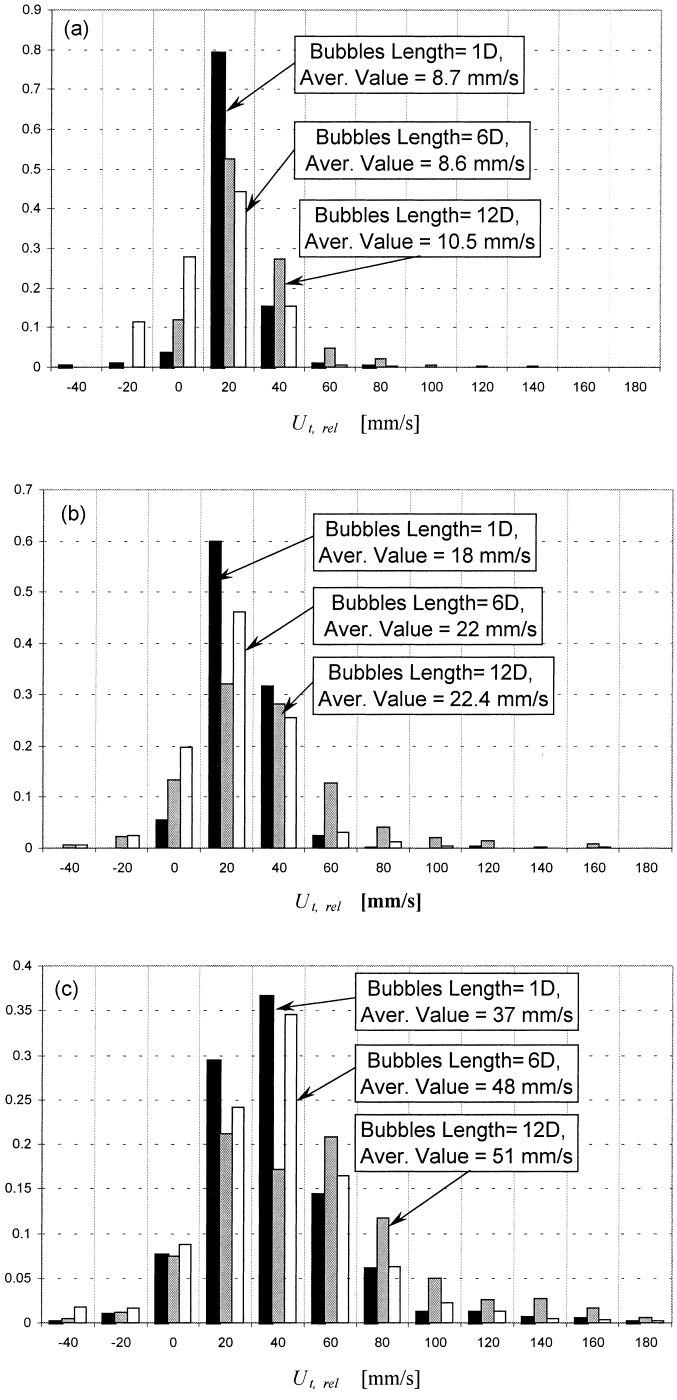

Fig. 14. Histograms of the instantaneous relative velocity of the trailing bubble for various bubble lengths.

is more pronounced for the longer bubbles. Even at considerable separation distances, the average velocity of the trailing bubble remains somewhat higher than that of the leading bubble. This effect is stronger for longer Taylor bubbles (Fig. 15b).

Fig. 16 presents the normalized average propagation velocity of the trailing Taylor bubble,

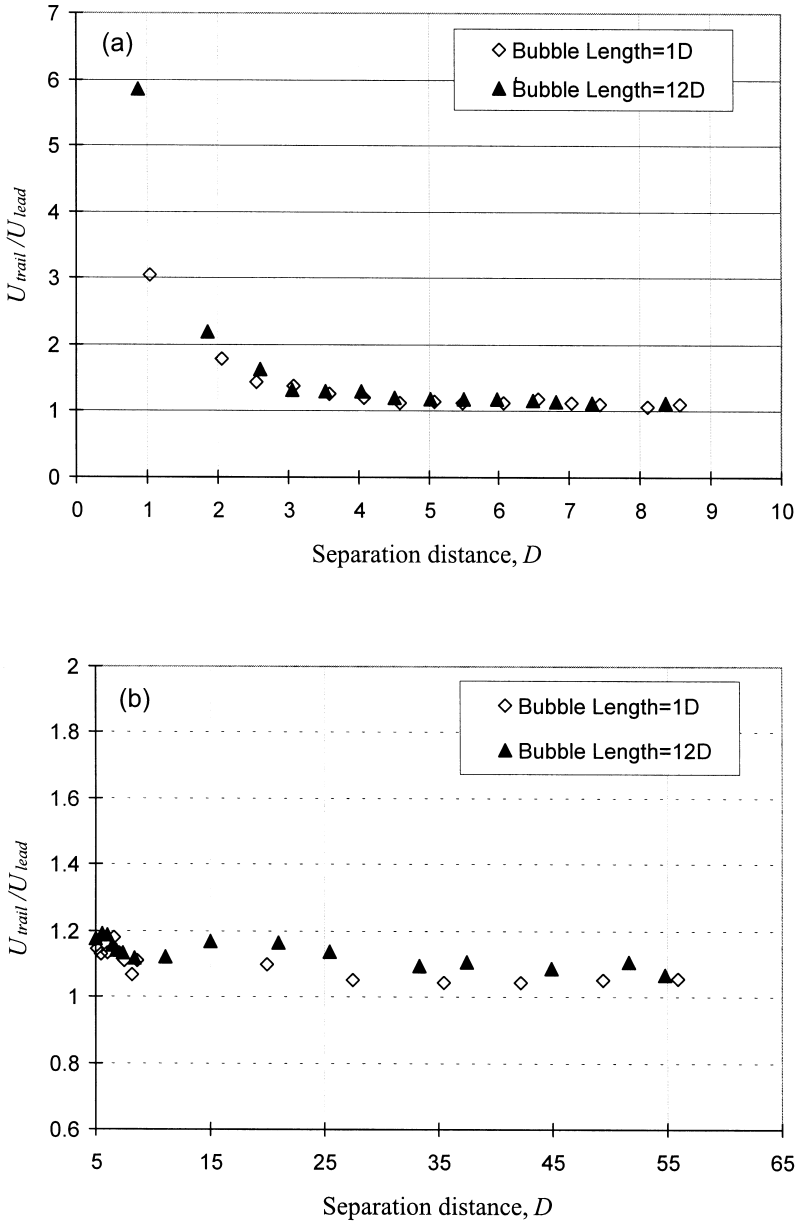

Fig. 15. Ratio of the averaged trailing bubble velocity to that of the leading one: (a) small separation distances, (b) large separation distances.

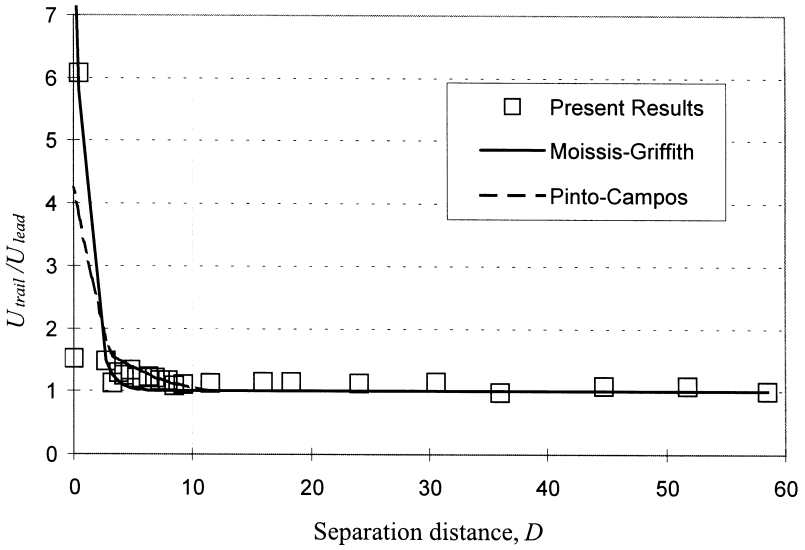

Fig. 16. Ratio of the averaged trailing bubble velocity to that of the leading one. Comparison with existing relations.

for the intermediate bubble length (about $6D$), as a function of the separation distances between the bubbles. The relation by Moissis and Griffith (1962), as well as the correlation of the experimental data by Pinto and Campos (1996) are also shown in this figure. At a distance of few pipe diameters, a considerable acceleration of the trailing bubble is obtained. In this region, the present results are close to those obtained earlier. The current measurements, however, extend to substantially larger distances than those investigated before. It appears that interaction between the bubbles exists at distances exceeding the generally assumed stable liquid slug length ($16D$ for a vertical flow). The present experimental results indicate an average rate of approach of $\sim$10 mm/s for distances between bubbles in the range of 60–$30D$.

4. Summary

Interaction between two consecutive Taylor bubbles rising in a stagnant liquid in a vertical pipe is studied quantitatively using the image processing technique. The applied technique allows one to follow closely and with high resolution the variation in space and time of various parameters of the bubble movement, such as the instantaneous shape of the interfaces, their locations and the propagation velocities. It thus became possible to extract not only the average flow parameters, but also the instantaneous values and their fluctuations. Strong deformation and oscillations of the trailing bubble tip were observed. It was shown that those oscillations are related to the quasi-resonant oscillations of the leading bubble bottom.

The oscillations in the tip location are accompanied by the corresponding temporal variation in the bubble propagation velocity. Certain ambiguity exists in the definition of the instantaneous propagation velocity of the trailing bubble in the near wake region due to those

effects. Considerable scatter in the experimental data in this region can be attributed in part to this ambiguity.

It was found here that the trailing bubble does not affect the motion of the leading one. The trailing bubble, on the other hand, is sensitive to the velocity distortion in the wake of the leading bubble. The trailing bubble acceleration is quite prominent in the near wake of the leading elongated bubble. In spite of this, instantaneous negative approach velocities are occasionally observed in this region. Even at distances exceeding 50 pipe diameters, the trailing bubble is affected by the vortical velocity field in the wake of the leading bubble. These results are of particular importance for the estimation of the stable slug length and for modeling transient slug flow.

It is quite clear that considerable further work on interaction of two consecutive bubbles in a vertical tube is required. In order to understand the quite complicated motion of the trailing bubble in the wake of the leading one, detailed measurements of the flow velocity in the liquid slug are required simultaneously with the measurements of the trailing bubble movement. These results stimulate future work on this problem using the Particle Image Velocimetry. Additional experiments are planned on bubbles moving in a flowing liquid, either upward or downward, as well as on elongated bubbles moving in more viscous liquids.

Acknowledgements

This work was partially supported by Tulsa University Fluid Flow Projects (TUFFP). The authors gratefully acknowledge this support.

References

Barnea, D., Brauner, N., 1985. Hold-up of the liquid slug in two phase intermittent flow. Int. J. Multiphase flow 11, 43–49.

Barnea, D., Taitel, Y., 1993. A model for slug length distribution in gas–liquid slug flow. Int. J. Multiphase flow 19, 829–838.

Bendiksen, K., 1985. On the motion of long bubbles in vertical tubes. Int. J. Multiphase Flow 11, 797–812.

Grace, J.R., Clift, R., 1979. Dependence of slug rise velocity on tube Reynolds number in vertical gas–liquid flow. Chem. Eng. Sci 34, 1348–1350.

Collins, R., de Moraes, F.F., Davidson, J.F., Harrison, D., 1978. The motion of a large gas bubble rising through liquid flowing in a tube. J. Fluid Mech 89, 497–514.

Davies, R.M., Taylor, G.I., 1949. The mechanics of large bubbles rising through extended liquids and through liquid in tubes. Proc. R. Soc. London Ser. A 200, 375–390.

Dumitrescu, D.T., 1943. Strömung an einer Luftblase im senkrechten Rohr. Z. Angew. Math. Mech 23, 139–149.

Fabré, J., Liné, A., 1992. Modeling of two-phase slug flow. Ann. Rev. Fluid Mech 24, 21–46.

Hasanein, H.A., Tudose, G.T., Wong, S., Malik, M., Esaki, S., Kawaji, M., 1996. Slug flow experiments and computer simulation of slug length distribution in vertical pipes. In: AIChE Symposium Series, Heat Transfer, Houston, 211–219.

Moissis, D., Griffith, P., 1962. Entrance effects in a two-phase slug flow. J. Heat Transfer, Trans. ASME C2, 29–39.

Netto, F.J.R., Fabré, J., Grenier, P., Péresson, L., 1998. An experimental study of an isolated long bubble in an horizontal liquid flow. In: Proc. 3rd Int. Conf. Multiphase Flow, Lyon, France.

Nicklin, D.J., Wilkes, J.O., Davidson, J.F., 1962. Two-phase flow in vertical tubes. Trans. Inst. Chem. Eng 40, 61–68.

Polonsky, S., 1998. Experimental study of hydrodynamic parameters in vertical upward slug flow. Ph.D. Thesis, Tel-Aviv University.

Pinto, A.M.F.R., Coelho Pinheiro, M.N., Campos, J.B.L.M., 1998. Coalescence of two gas slugs in a co-current flowing liquid in vertical tubes. Chem. Engng. Sci. 53, 2973–2983.

Pinto, A.M.F.R., Campos, J.B.L.M., 1996. Coalescence of two gas slugs rising in a vertical column of liquid. Int. J. Multiphase Flow 51, 45–54.

Polonsky, S., Barnea, D., Shemer, L., 1999a. Averaged and time-dependent characteristics of the motion of an elongated bubble in a vertical pipe. Int. J. Multiphase Flow 25, 795–812.

Polonsky, S., Shemer, L., Barnea, D., 1999b. An experimental study of the relation between the Taylor bubble motion and the velocity field ahead of it. Int. J. Multiphase Flow 25, 957–975.

Shemer, L., Barnea, D., 1987. Visualization of the instantaneous velocity profiles in gas–liquid slug flow. Physicochem. Hydrodyn 8, 243–253.

Taitel, Y., Barnea, D., 1990. Two-phase slug flow. Adv. Heat Transfer 20, 83–132.

Taitel, Y., Barnea, D., Dukler, A.E., 1980. Modeling flow pattern transitions for steady upward gas–liquid flow in vertical tubes. AIChE J 26, 345–354.

Van Hout, R., Shemer, L., Barnea, D., 1992. Spatial distribution of void fraction within a liquid slug and some other related slug parameters. Int. J. Multiphase Flow 18, 831–845.

Zheng, G., Brill, J.P., Taitel, Y., 1994. Slug flow behavior in a hilly terrain. Int. J. Multiphase Flow 20, 63–79.